

Women in Aerospace

University of Illinois at Urbana Champaign



Team mentor: Jonathan Sivier

Faculty Adviser: Diane Jeffers

dejeffer@illinois.edu 217-244-8048

Team Lead: Michal Silezin

silezin2@illinois.edu 630-965-5821

Team members

Alexandra Bacula

Matthew Koll

Emlee Ballowe

Courtney Leverenz

Katherine Carroll

Natalie Pfister

Megan Geyer

TABLE OF CONTENTS

EXECUTIVE SUMMARY	ii
1. MECHANICAL AND ELECTRICAL DESIGN.....	1
1.1 Overall Dimensional Specifications.....	1
1.2 Rocket Airframe Design Features.....	1
1.2.1 Motor Selection and Propulsion System Specifications.....	1
1.2.2 Upper Airframe	4
1.2.3 Coupler	4
1.2.4 Booster Airframe.....	5
1.2.5 Recovery System	5
1.3 Electronic and Payload Design Features	6
1.3.1 Active Drag System	6
1.3.2 Avionics	7
1.3.3 Velocity Measurement System	7
1.4 Construction Process	8
1.5 Structural Analysis of Scratch Built Parts	10
1.6 Risk Mitigation Analysis	10
2. PREDICTED PERFORMANCE	11
2.1 Launch Analysis	11
2.2 Flight Analysis	11
2.2.1 Estimated Maximum Altitude	11
2.2.2 Estimated Peak Velocity	13
2.2.3 Estimated Drag Coefficient	15
2.3 Recovery Analysis	17
2.4 Stability Analysis	17
2.5 Environmental Conditions Analysis	18
3. SAFETY	19
3.1 Flight and Recovery Safety	19
3.2 Material-Handling Procedures	19
3.3 Assembly Procedures	19
3.4 Pre- and Post-Launch Procedures	20
4. TEST FLIGHTS	20
4.1 Model Rocket Demonstration Flight	20
4.2 Test Flight Plan	21
5. BUDGET	21

Executive Summary

The rocket, active drag system, and velocity measurement device were all designed with simplicity and reliability in mind. The rocket will primarily be made out of Blue Tube for the main body, a polypropylene plastic nose cone, and fiberglass fins. The materials were chosen due to their light weight, high strength, and low cost, making them practical and reliable options for the team. The rocket's active drag system was designed to deliver a constant, failure-proof, source of drag. The design consists of two solenoid locks, a microcontroller, torsion springs, two fiberglass fins, and an aluminum rod containing metal stoppers offset at 90 degrees. The two solenoids will alternate releasing the stoppers to produce quarter rotations of the fins, alternating between vertical and horizontal configuration. The velocity measurement system will consist of a pitot probe and pressure transducer interfaced with an arduino microcontroller. The system will use readings of the static and dynamic pressures during the rocket's ascent to calculate velocity. The team's goals for the competition are to design and build a functional system that meets competition parameters, is reliable and performs to high standards, and to obtain relevant data during the flights that will enable analysis and evaluation of system performance.

1. MECHANICAL AND ELECTRICAL DESIGN

1.1 Overall Dimensional Specifications

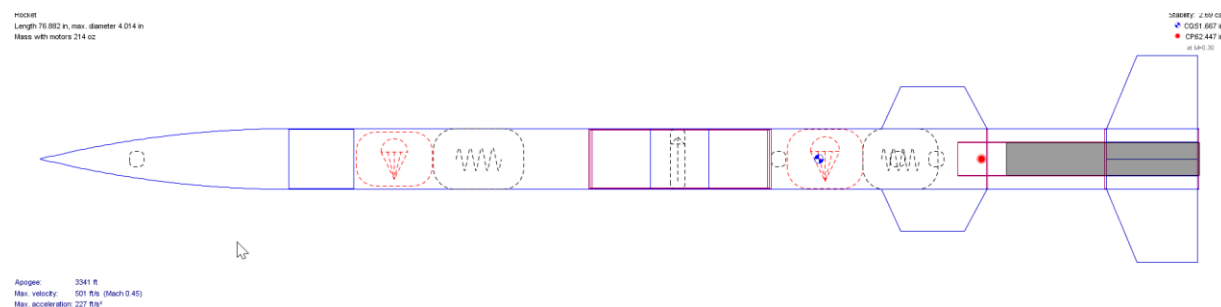


Figure 1. OpenRocket diagram before motor burnout.

The total length of the rocket is 6.41 ft with an outer diameter of 4.01 in. It consists of a nose cone, upper airframe section, coupler section, and booster section. The total weight of the rocket, including the full weight of the motors, is 14.18 lbs with one motor and 13.81 lbs with the other. The center of pressure is denoted by a red dot on Figure 1 and is located 5.02 ft from the tip of the nose cone, or 1.39 ft from the base. The center of gravity is denoted by a blue and white dot on Figure 1. The center of gravity is dependent on time due to mass loss from the motor burning. Additionally, since each motor that has a different mass, the center of gravity is dependent on motor choice. The motors that have been chosen are the Cesaroni J295-16 and Cesaroni K2045Vmax-17.

Using the J295-16 motor, which has a launch weight of 2.47 lbs, the center of gravity prior to motor burnout is located 4.36 ft from the tip of the nose cone, or 2.05 ft from the base of the rocket. Once motor burnout occurs at 4.03 seconds, the center of gravity shifts to 4.2 ft from the tip of the nose cone, or 2.21 ft from the base. After motor burnout occurs, the location of the center of gravity remains constant during flight before the recovery device deploys.

For the second launch, the K2045Vmax-17 motor will be used, which has a slightly greater launch weight of 2.84 lbs. The center of gravity using this motor is initially located 4.37 ft from the tip of the nose cone, or 2.04 ft from the base before motor burnout. Once the motor burnout occurs at 0.776 seconds, the center of gravity moves to 4.2 ft from the tip of the nose cone, or 2.21 ft from the base. Comparing the two results, it can be noted that the weight of the two motors was intentionally chosen to be very similar so that the center of gravity does not drastically change between launches. Additionally, the centers of gravity after each motor burnout match at 4.2 ft from the tip of the nose cone, ensuring our simulations are accurate.

1.2 Rocket airframe design features

1.2.1 Motor Selection and Propulsion System Specifications

The motors were chosen to maximize the ability to achieve competition goals while minimizing the possibility of rocket failure. Both “J” and “K” class rockets were considered to best meet competition requirements. The team decided to only consider motors of class “J” and

“K” due to the weight of the rocket and making sure that the minimum apogee of 3,000 ft is achieved. Motors from Cesaroni Technology Incorporated and AeroTech were considered in this design. After initial analysis, a rocket diameter of 4.01 in was chosen, so all of the motors that were considered were 54 mm to account for this diameter.

From those parameters, a set of motors was chosen that allowed the rocket to reach the highest altitude possible while yielding the highest score according to the scoring formula, shown below.

$$\text{Figure of Merit (FM)} = \text{Apogee}_{avg} * \frac{\left(\frac{\text{Total Impulse}_{max}}{\text{Total Impulse}_{min}}\right) * \left(\frac{\text{Avg Thrust}_{max}}{\text{Avg Thrust}_{min}}\right)}{\left(\frac{\text{Apogee}_{max}}{\text{Apogee}_{min}}\right)^2 * \left(\frac{\text{Initial mass}_{max}}{\text{Initial mass}_{min}}\right)} \quad (1)$$

and

$$70 * \left(\frac{FM_{your\ rocket}}{FM_{competition\ max}} \right) \quad (2)$$

All of these motors were checked to ensure they would allow the rocket to exceed the required 45 ft/s at 8 ft off the ground. Due to the large impulse and short burn time of the K2045Vmax-17 motor, this was considered the optimum “K” class motor to maximize score while still being safe to fly. Several “J” class motors were considered. These rocket motors are summarized in Table 1 below. Additionally, a compilation of the respective motor Figure of Merits is shown in Table 2 below.

Table 1. Motor Data Comparison

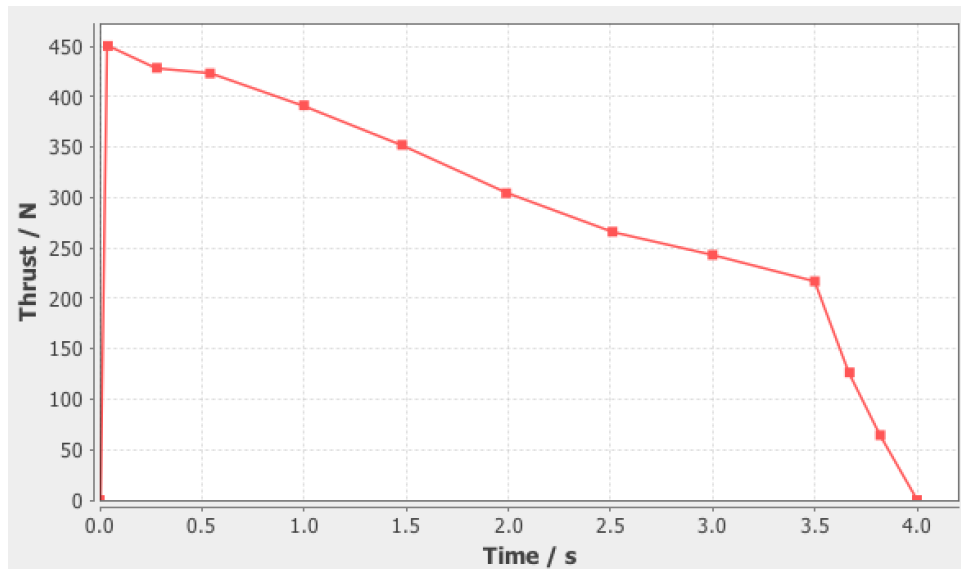
Motor	Apogee (ft)	Rail Exit Velocity (ft/s)	Maximum Velocity (ft/s)	Maximum Acceleration (ft/s ²)	Motor Burn Time (s)	Launch mass (lbs)	Impulse (Ns)	Maximum Thrust (N)
J295-16	3557	56.9	474	203	3.94	2.47	1196	451
J325TT-P	3057	60.3	437	244	3.3	2.71	1089	541
J415W-6	3572	58.9	496	244	3.37	2.64	1201	552
J401FJ-6	3333	59.2	501	229	2.69	2.02	1108	488
K2045Vmax-17	4452	127	721	1118	.709	2.84	1417	2184

Table 2. Figure of Merit Value Table

J Motor (Paired with K2045Vmax-17)	Motor Dependent Figure of Merit Values
J295-16	22,368
J325TT-P	19,548
J415W-6	18,481
J401FJ-6	21,003

As can be seen above, the J295-16 yielded the highest Figure of Merit value based on average apogee, thrust ratio, impulse ratio, and mass ratio. The actual difference in apogee depends on the active drag system and was consequently not included in the calculation. The J295-16 and K2045Vmax-17 are therefore the best motor choices to maximize score.

The Cesaroni J295-16 is a reloadable motor that is 54 mm (2.13 in) in diameter and 329 mm (13 in.) in length. It has a burn time of 3.94 s and an ejection charge delay of 16 s. It has an average thrust of 304 N and a maximum thrust of 451 N occurring at 0.04 s. The thrust curve can be seen below in Figure 2 and the total impulse is 1196 Ns. The launch mass of the motor is 2.47 lbs and the mass after burnout is 1.16 lbs.

**Figure 2. Thrust curve for the Cesaroni J295-16.**

The Cesaroni K2045Vmax-17 is a reloadable motor that is 54 mm (2.13 in) in diameter and 404 mm (15.9 in) in length. It has a burn time of 0.7 s and an ejection charge delay of 17 s. It has an average thrust of 1996 N and a maximum thrust of 2184 N occurring at 0.3 s. The thrust curve can be seen below in Figure 3. The total impulse is 1417 Ns. The launch mass of the motor is 2.84 lbs and the mass after burnout is 1.26 lbs.

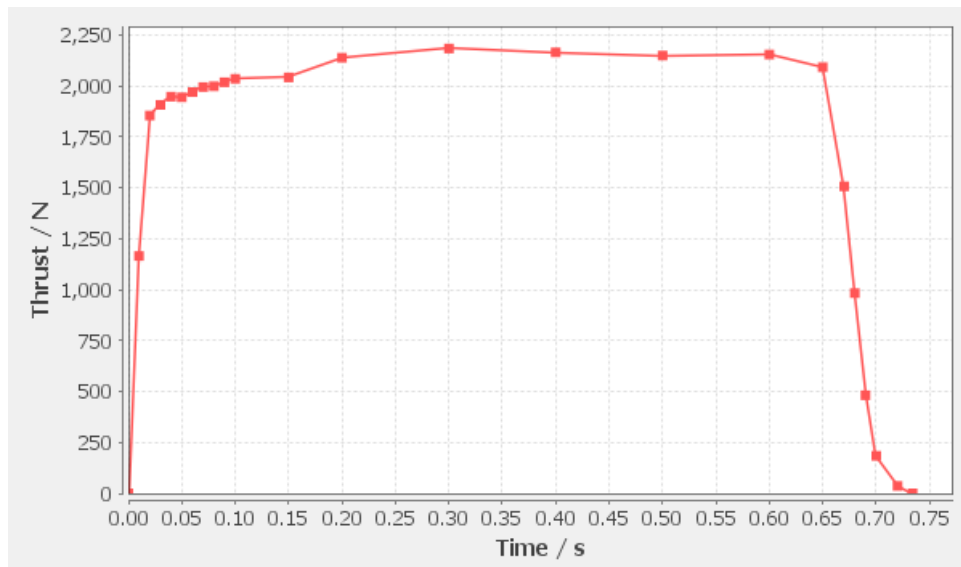


Figure 3. Thrust curve for the Cesaroni K2045Vmax-17.

1.2.2 Upper Airframe

The upper airframe consists of the nose cone, a Blue Tube section, the main parachute, shock cords, quick links, parachute protectors, and all the components of the velocity measurement system. The nose cone has an ogive profile, a shoulder length of 3.25 in, an outer diameter of 4 in and is 16.5 in long. It is made out of polypropylene plastic and weighs 0.652 lbs. The nose cone will house the pitot-static probe and arduino. The tip of the nose cone will be removed to allow the probe to protrude. The Blue Tube section connected to the nose cone is 2 ft in length and weighs 0.793 lbs. This Blue Tube section holds the main parachute and its peripherals. The main parachute will be attached to an eye bolt at the base of the upper airframe. On the bulkhead separating the upper airframe and the coupler will be an ejection charge to deploy the main parachute. Potential airframe and general body material choices included fiberglass, Blue Tube, and carbon fiber. Blue Tube was chosen due to it being relatively inexpensive and strong. While carbon fiber would have been the best material choice due to it being lighter and stronger than both Blue Tube and fiberglass, it can be hazardous to work with and is more expensive. Fiberglass is stronger than Blue Tube, but it is also twice as heavy. The additional strength is not necessary; however, because Blue Tube is rated high enough to withstand the loads encountered during the mission. Blue Tube's shatterproof nature also increases the reusability and safety of the rocket.

1.2.3 Coupler

The coupler section consists of a 12 inch long section of Blue Tube and houses the avionics and bulkheads. A Blue Tube switchband is centered on the outside of the coupler measuring 4 inches in length with an outer diameter of 4.01 in to create space between the upper airframe and booster section while reinforcing the connection point of the two coupler sections.

The two bulkheads at the end of the coupler are made out of 0.25 in thick plywood, have an outer diameter of 3.73 in, and each weigh 0.115 lbs. These will serve as an attachment point for the eye bolts to attach the main and drogue parachutes.

1.2.4 Booster Airframe

The booster airframe consists of a 4.01 in section of Blue Tube measuring 2.71 ft in length. The drogue parachute and its accessories are inside this airframe. The drogue will be attached to an eyebolt located on the outer side of the coupler's bulkhead, as well as the upper centering ring. The outside of the booster airframe will house the active drag system. Two sets of drag fins and solenoids will be placed symmetrically on either side of the airframe. In addition, the booster airframe will house the motor, fixed with the motor mount and motor retainer, which will be held in place by three centering rings made of plywood as well as an aft enclosure. On the outside of the booster airframe are four fiberglass fins made out of 0.125 in thick fiberglass. They will be spaced equally around the rocket, each with a span of 4.85 in measuring 4 in at the tip and 6 in at the root. The fins will be epoxied to the body tube as well as to the motor mount tube inside of the body tube for additional support. Along the outside of the airframe will be two 1515 rail buttons made out of Delrin-plastic with a length of 0.68 in and an outer diameter of 0.63 in. Rail buttons will ensure that the rocket leaves the launch rail in the desired direction.

1.2.5 Recovery System

The recovery system of the vehicle will be comprised of an 18 in drogue parachute stored in the booster section and a 60 in main parachute housed in the upper airframe. Other components included in the recovery system consist of tubular nylon shock cords, parachute protectors, quick links, eye bolts, shear pins, and an ejection charge. The sizes of the drogue and main parachute were determined through various simulations in OpenRocket and from the experience of the team mentor. The 18 in drogue parachute is made out of ripstop nylon, weighs 0.041 lbs, and has a drag coefficient of 0.80. The 60 in main parachute is made out of silicone-coated ripstop nylon, weighs 1.2 lbs, and has a drag coefficient of 1.89. The main parachute is attached to a 15 ft tubular nylon shock cord weighing 0.161 lbs. The shock cord is then attached to two quicklinks, which are hooked onto an eye bolt. The eye bolt will be screwed into the coupler and secured by washers and a nut. The ejection charges are located on the sides of the bulkheads facing out of the coupler. The ejection charge for the drogue will have one gram of black powder, while the ejection charge for the main parachute will have two grams of black powder. The amount of black powder was determined using an online black powder ejection charge calculator which took into account the diameter and length of the section in which the parachute is stowed, as well as the pressure needed for successful parachute ejection, which is typically 10 to 15 psi for a 4 in diameter rocket.

1.3 Electronic and Payload Design Features

1.3.1 Active Drag System

The active drag system consists of two rotating fins located 21 in from the base of the rocket. The fins will have a trapezoidal shape with a root chord of 7 in and tip chord of 5 in. They will be 2.7 inches wide and will be constructed out of fiberglass that is 0.125 in thick. The rotation point of the fins is located about 5 in below the center of gravity of the rocket after motor burnout for both motors. A CAD model of the active drag system can be seen in Figure 4.

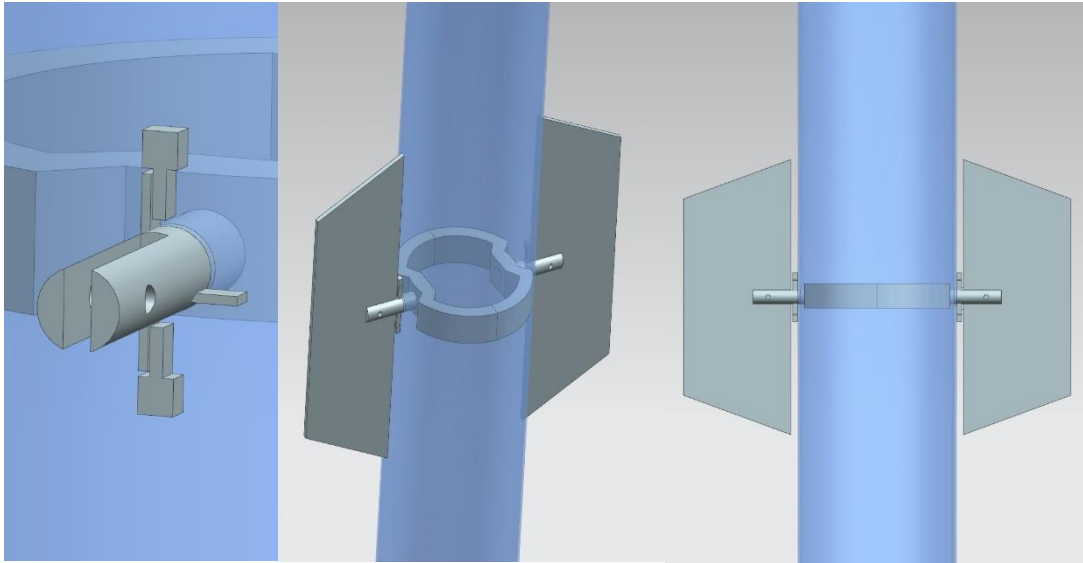


Figure 4. Three views of the CAD model of the active drag system.

When not activated, the fins are stowed such that they run parallel to the rocket body in order to reduce drag. The drag system will be activated after motor burnout and will be deactivated and returned to initial configuration before apogee. Upon activation, the fins will pivot 90° on their center axis becoming aligned perpendicular to the body tube. This will increase the surface area and consequently the drag on the rocket. The fins and attachments will be sturdy enough that they will not fracture or tear off the rocket body when activated.

Each fin of the active drag system will be attached to a rod running into the rocket and attached along the centerline of the rocket. Each rod will have three protrusions offset by 90° . These protrusions will be used in conjunction with solenoid locks to rotate the fins in 90° intervals. Torsion springs will help facilitate the rotation of the rods in opposing directions. This will prevent the rocket from drifting laterally and, more importantly, from tumbling about the lateral axis as the fins rotate. By turning the fins in opposite directions, stability will be maintained and the rocket will not break apart as the active drag is applied. The solenoids will be secured to the outside of the booster frame.

When motor burnout occurs, the bottom solenoid will be released to permit the rod to rotate 90° and be stopped by the top solenoid. At apogee the bottom solenoid will be activated again and the top released. This will once more allow the fins to rotate 90° . The solenoids will be powered by a 9V battery and the solenoid releases will be triggered by an arduino and Raven3 altimeter according to acceleration data.

1.3.2 Avionics

The avionics system will be included in the coupler section of the body tube. The avionics bay will be in the bottom half of the coupler section taking up approximately 6 inches in length. It will be separated from the bottom booster section and upper active drag component with a bulkhead.

Components of the avionics system include two threaded rods and a plywood sheet for the avionics bay, two altimeters, two 9V batteries, two switches, three terminal blocks, and wires. A rectangular piece of plywood will act as the avionics sled. This will be the platform on which all of the avionics will be secured. It will have two rows of small 3D printed tubular guides epoxied to the plywood each a few inches apart. The threaded rod will be passed through these guides to attach the avionics bay to the bulkheads that will go on the end of the avionics coupler section.

On the avionics bay, one Raven3 altimeter and two Stratologgers will be screwed on and two 9V battery holders will either be epoxied or screwed on. Since the Stratologger covers dual-deployment, one will fire the main charge for the main and drogue parachute. The second Stratologger will fire the backup charge for the main parachute. No backup from the Stratologger is needed for the drogue parachute because the motor charge will serve as the backup. Wires will connect the Stratologgers to the charges, battery, and switches.

The Stratologgers will have independent switches to arm and disarm them. The rotary switches will be passed through a hole in the body tube of the coupler section and will be screwed in with a nut. One switch will control the main charge Stratologger while the other will control the backup charge Stratologger. Each switch will be clearly labeled as to which Stratologger it controls, which position is on and which position is off. The switches will be turned using a flathead screwdriver.

Wires from the ports of the Stratologger named drogue and main will be led through the coupler and bulkhead to the outside of the bulkhead. They will then be connected to the terminal block which is connected to the black powder charges on the other end. Using these terminal blocks makes assembly of the coupler and charges easier.

There will also be a pressure sensor on the avionics bay. The pressure sensor will be screwed on similar to the Stratologgers. It will be used to take measurements of the coefficient of drag during flight. This data will be used post flight to create a model of the active drag system.

Additionally, there will be two small microHD cameras on the bay, one facing upwards and one facing downwards. The cameras will be attached to the side of the rocket with a balsa wood camera shroud. These cameras are ideal because they are lightweight while also being durable and weather/water resistant. These cameras will allow the operation of the active drag to be filmed. With this footage the team will be able to see the movement of the active drag fins, which allows for better evaluation of the performance and allows for easier troubleshooting if something were to go wrong in the operation of the system. The footage also provides comparison points with the data collected during flight. The data gathered from the pressure sensor can be compared to the video to see what physically changed during active drag operation to affect the coefficient of drag.

1.3.3 Direct Velocity Measurement System

A pitot/static transducer with a Prandtl tube will be used for the direct velocity measurements. The OpenRocket simulation shows that the maximum velocity of the rocket when using the K2045Vmax-17 motor is 720 ft/s. This can be converted into a mach number of 0.65

when using the speed of sound at standard conditions. The isentropic relation for static pressure and stagnation pressure show that the minimum pressure ratio will be 0.75. This pressure ratio is then used to determine the maximum pressure difference the rocket will be under during flight. Assuming the ambient air pressure, 14.7 psi, as the static pressure, the stagnation pressure will be 19.5 psi. This means that the pressure transducer will have to be able to measure a pressure differential of at least 4.8 psid. The effects of temperature on the speed of sound have been considered. However, assuming the OpenRocket apogee is correct, the change in speed of sound due to temperature is less than 15 ft/s. This turns out to be two percent of the maximum velocity expected by OpenRocket. Thus, the effects temperature has on the speed of sound are being considered negligible.

1.4 Construction Process

The construction of the rocket will be broken down into various sections that will take place throughout the second half of the spring semester. All parts necessary for manufacturing and assembly were ordered in early February and were delivered in mid-February. Construction of each section is scheduled to begin on March 11th. Team members will not be allowed to work alone, and must always work in groups of two or more. This is to help minimize risks in the lab and is also a result of the rules of the workspace in which the rocket will be built.

Upon receipt, all parts have been inventoried, inspected, weighed, cleaned, and labeled. Before permanently attaching any components, the rocket will be dry assembled as fully as possible to make sure that each manufactured part fits the correct dimensions. General construction practices will include marking all hole locations, confirming hole and insert sizes, and reaffirming locations before drilling or fastening with epoxy. Basic construction tools and supplies include but are not limited to an X-Acto knife, a drill and bits, a Dremel tool, a soldering iron, and a palm sander. High strength epoxy will be used for bonding major areas of the flight vehicle. Surfaces that will have epoxy applied will be sanded with 60 grit or lower sandpaper and will be later cleaned with rubbing alcohol. The amount of epoxy applied will be determined by the structural integrity and consequential drag effects while in flight. Hazards associated with exposure to epoxy have been addressed and actions taken to mitigate risk are noted in Section 1.6.

Construction of the rocket will begin with the motor mount. Three centering rings made of 0.25 in plywood will be used for structural support and ease of alignment. The location of the centering rings will be marked on the motor mount and body tube in three different locations: the top ring slightly below the top of the motor mount tube, the middle ring aligned with the top of the fins, and the bottom ring aligning the retainer with the bottom of the rocket. Motor retention will be ensured by an Aero Pack 54mm motor retainer constrained at the extreme aft end of the rocket.

Next, rail button positions will be marked on the airframe and attached before the motor mount is fixed inside of the rocket. To secure the rail buttons, T-nut interfaces will be created on

the inside of the rocket. The interfaces will consist of a T-nut inserted into a block of plywood and will be mounted to the top and bottom centering rings. Next, the inside of the booster airframe and the fin slots will be sanded. Epoxy will be applied to the top of the aft centering ring, through a hole for the top ring, and through a fin slot for the middle ring. The motor mount will be inserted into its marked location in the booster airframe at a later time.

Another component of the construction process is assembling the avionics bay. All electronics will be carefully attached to assigned locations on the avionics sled and appropriate electrical hardware will be used to make sure that no wires are left exposed. Threaded rods will be attached to the bulkhead and run the length of the avionics bay to act as guide rails for the avionics sled as it is inserted into the airframe. The avionics sled will have two hollow tubes attached to the sides lengthwise. The threaded rods are able to slide into the hollow tubes, securing the avionics bay in place. The bulkheads of the avionics bay will also have the charge cups, terminal blocks, and eyebolts for parachutes attached to them.

The trapezoidal fins will be carefully constructed out of 0.125 in fiberglass and will be in a through-the-wall configuration. Upon construction, fin alignment will be ensured through the use of a simple jig consisting of slots placed 90° apart. When affixing the fins, a generous amount of epoxy will be applied between the fins and the body tube for support, making sure that no residue is left to create undesirable drag consequences. Internal fillets for the fins will assure that the fins fit tight to the motor mount tube and that the centering rings fit snug to the top and bottom of the fins.

The active drag system of the rocket will be constructed by first 3D printing a mounting ring. The mounting ring will then be epoxied into the inside of the booster airframe. The rods with mounted torsion springs will then be secured to the inside of the airframe onto the ring. The solenoid locks will be epoxied into their respective positions on either side of the mounted rod. The system will be completed by hooking up all required connections between the solenoids, batteries, and arduino. Construction techniques are subject to change as the team approaches obstacles in the manufacturing process.

Verification of the vehicle construction will be accomplished as components are completed by experienced team members and the team mentor. These individuals will inspect all connections and other construction features to ensure that the manufacturing process proceeds as planned and provides for sufficient structural integrity. Additionally, each time a component is completed, its integration with other completed parts will be tested. Inspecting components as they are completed will allow the team to catch any errors or defects as early as possible, and resolve the problems as they arise. The building process will conclude with priming and painting the exterior for aesthetic appeal and drilling pressure relief holes in the airframe to allow pressure to equalize in flight.

1.5 Structural Analysis of Scratch Built Parts

The majority of the rocket is scratch built, so it is integral the components are structurally sound. The main body tube will be put under many forces during flight and recovery so the team chose to use Blue Tube due to its durability and high strength. Blue Tube is shatterproof, eliminating the worry of the body tube breaking and splintering under stress or impact. Team members have flown many rockets with great success using Blue Tube as the main body tube. The aerodynamic and active drag fins will be made of fiberglass due to its high strength. While they are heavier, the fiberglass will be able to withstand the forces of flight and the impact of landing reliably. The fins are attached through the body tube to the motor mount, adding extra assurance that they will be able to withstand flight and landing conditions. The epoxy used to hold on the fins is strong enough to secure the fins to the body tube, while being elastic enough to bend slightly as force is put on the fins during flight. Epoxy will also be used to hold together the coupler. The epoxy will create a strong bond joining the two sections of coupler and will be able to withstand the forces of launch and landing. The avionics sled will be manufactured out of plywood due to its low weight and relatively high strength, allowing it to hold all avionics securely without compromising weight.

1.6 Risk Mitigation Analysis

When constructing a rocket, there are many potential hazards that must be predicted and accounted for. To ensure safe habits in the construction process, the team must be prepared to address these risks. In Table 3 below, possible risks are listed, as well as how the team plans to prevent the risk.

Table 3. Risk Mitigation

Possible Risk	Mitigation Solution
Skin contact with epoxy	Wear gloves at all times when handling epoxy
Power tool accidents	All team members will be trained on power tools by experienced instructors--safety equipment such as safety glasses and earplugs will be worn throughout the build process
Inhaling fiberglass	Wear masks during the cutting of fiberglass
Inhaling epoxy fumes	Use proper ventilation in student workspace and wear masks if necessary
Black powder explosion	Black powder, along with all other explosives, will be stored very carefully according to their safety instructions
Electrical Shock	All wiring will be thoroughly checked and

	tested to ensure the connections are correct before supplying power
Foreign objects in eye(s)	Wear safety glasses while cutting fiberglass or working with anything else that may create small particles

2. PREDICTED PERFORMANCE

2.1 Launch Analysis

Using the model rocket simulator OpenRocket, the rocket launch performance was simulated in order to predict the rocket's performance before actually building and flying. This was done using both the K2045Vmax-17 and J295-16 motors with active drag disengaged. When active drag is engaged, a custom made simulation must be used to predict the rocket's performance. The simulation used an 8 ft launch rail set vertically at 0 degrees. In order to meet competition requirements, the launch rail departure velocity at 8 ft must exceed 45 ft/s.

When analyzing the K2045Vmax-17 motor, the rail exit velocity will be 127 ft/s which far exceeds competition requirements. The rocket will clear the launch rail at 0.139 s, with a vertical acceleration of 1025 ft/s^2 and stability margin of 2.16. At 0.7 seconds, shortly before motor burnout, the rocket will reach its peak velocity of 720 ft/s. Motor burnout will occur at 0.748 s, at which time the rocket will be at an altitude of 287 ft, a vertical velocity of 717 ft/s, a vertical acceleration of -112 ft/s^2 , and a stability margin of 3.09.

For the J295-16 motor, the rail exit velocity will be 56.9 ft/s, which also exceeds the requirements. The rocket will clear the launch rail at 0.31 s, with a vertical acceleration of 193 ft/s^2 and stability margin of 1.82. At 3.98 s, shortly before motor burnout, the rocket will reach its peak velocity of 464 ft/s. Motor burnout will occur at 4.03 s, at which time the rocket will be at an altitude of 1218 ft, a vertical velocity of 461 ft/s, a vertical acceleration of -63.1 ft/s^2 , and a stability margin of 3.01.

2.2 Flight Analysis

2.2.1 Estimated Maximum Altitude

The estimated maximum altitude of the rocket was simulated using OpenRocket. Based on data from past flights, the simulations have routinely overshoot the actual altitude by about five percent, so a slightly lower apogee is expected in flight. The first flight will be using the Cesaroni J295-16 motor to gather our target apogee. Using the OpenRocket simulation, the rocket is expected to reach 3556 ft apogee at a time of 15.5 s using the J295-16 motor. A plot with the OpenRocket simulation with event markers can be seen in Figure 5.

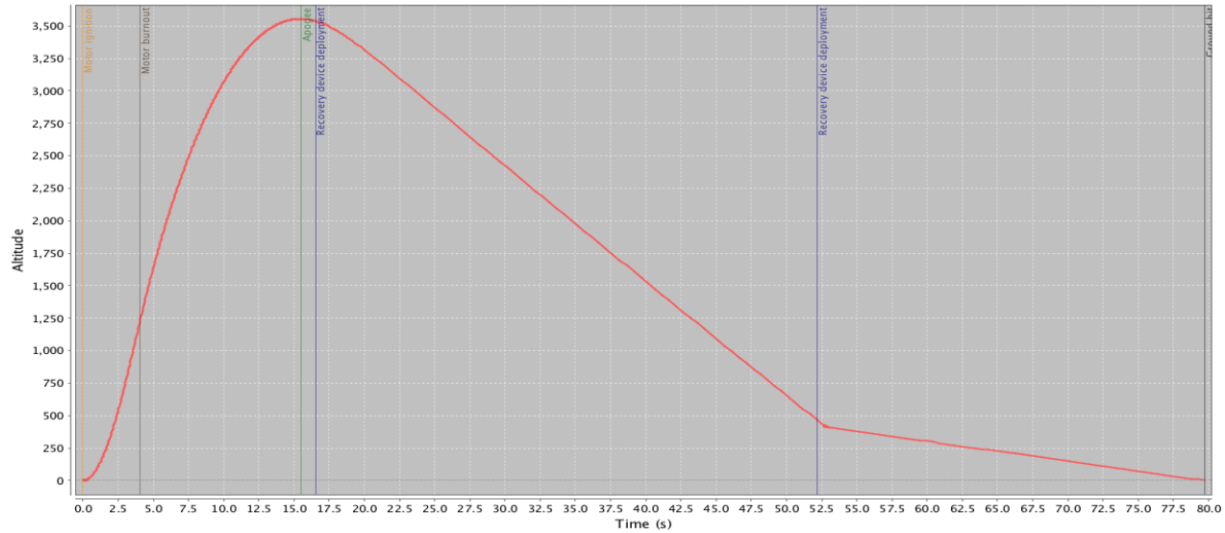


Figure 5. OpenRocket altitude simulation for the J295-16 with active drag stowed.

While the launch with the Cesaroni K2045Vmax-17 will be disturbed by engaging the active drag system, it is important to understand how the rocket would behave with the drag fins stowed. It is essential to know the difference between target apogee and what would occur without the active drag system engaged. Using the OpenRocket simulation with drag fins stowed, the rocket is expected to reach a 4448 ft apogee at a time of 15.4 s. A plot with the OpenRocket simulation with event markers can be seen in Figure 6.

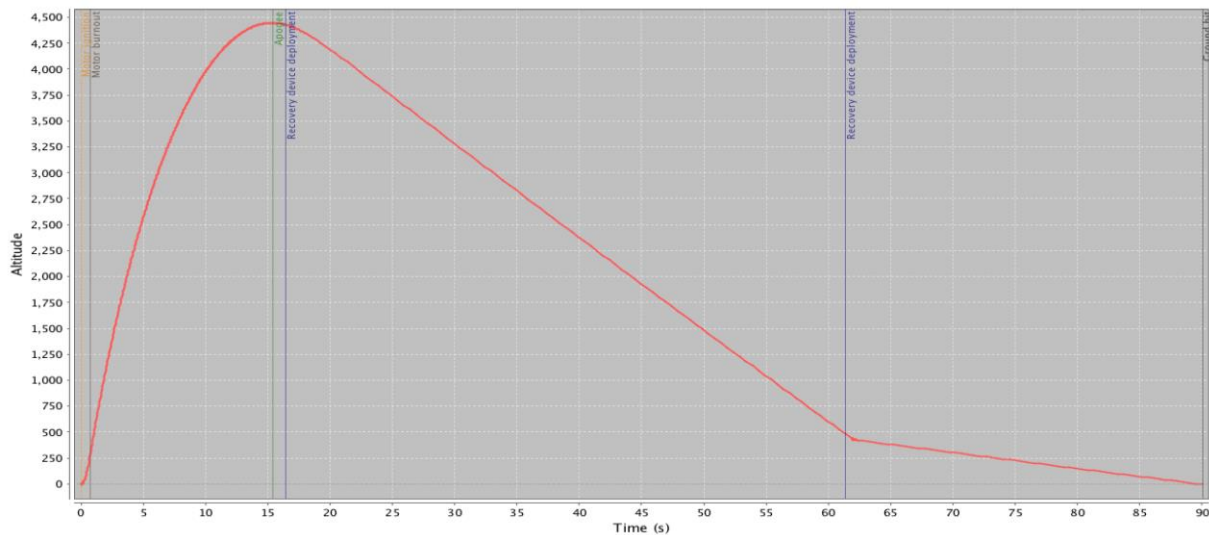


Figure 6. OpenRocket altitude simulation for the K2045Vmax-17 with active drag stowed.

Unfortunately, OpenRocket does not have the capabilities to accurately model active drag, so the team will rely on the custom simulation to accurately predict its flight. This

simulation will be compared to the data gathered from the rocket's test flight and verified to ensure its accuracy. The custom simulation currently has the rocket reaching an altitude of 3051 ft with active drag engaged using the K2045Vmax-17 motor. A plot of the altitude versus time for the rocket with the active drag system enabled, along with a comparison to the altitude plot with active drag stowed, can be seen in Figure 7.

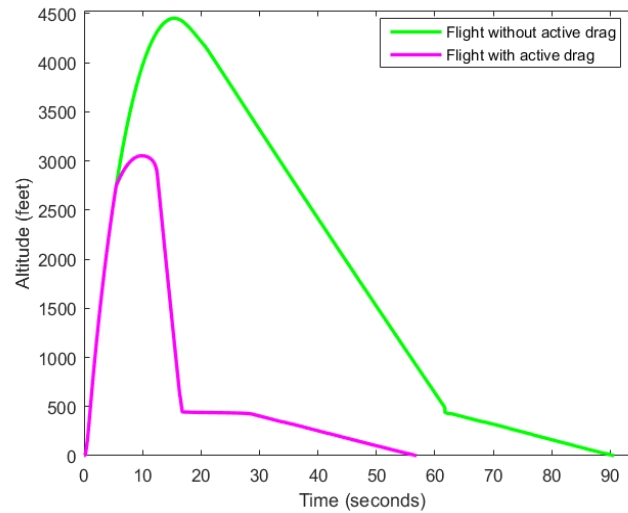


Figure 7. OpenRocket altitude simulation for the K2045Vmax-17 with active drag engaged.

2.2.2 Estimated Peak Velocity

The estimated peak velocity was also simulated using both OpenRocket and the custom simulation program. OpenRocket works well to model the peak velocity during the flight without the active drag being utilized. The peak velocity, as shown by the OpenRocket simulations, is 472.89 ft/s using the J295-16 motor and is achieved near motor burnout as expected. The plot of the OpenRocket simulation of velocity versus time using the J295-16 motor with active drag stowed can be seen below in Figure 8.

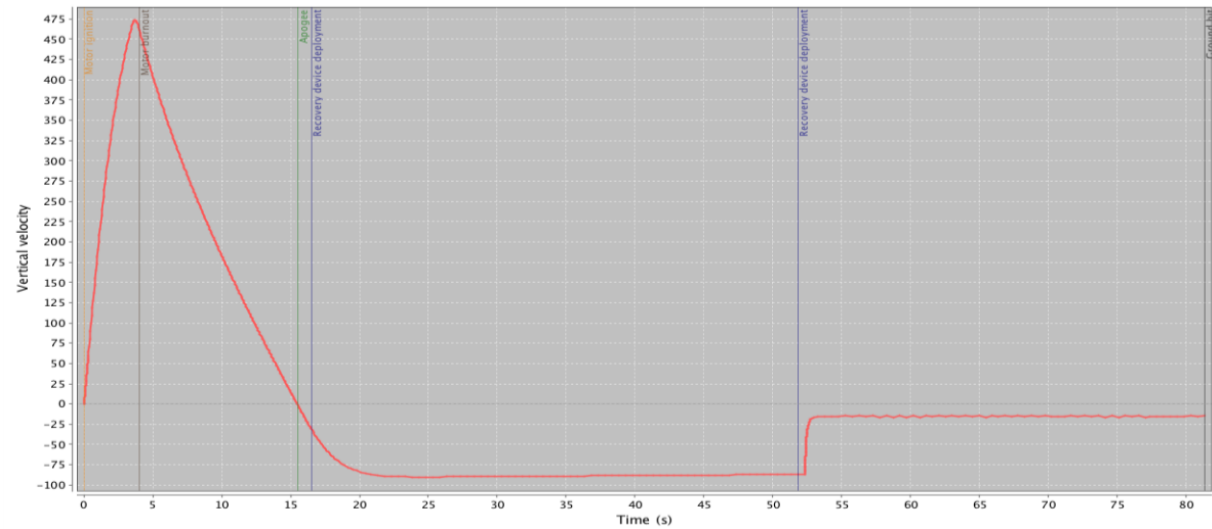


Figure 8. OpenRocket velocity simulation for the J295-16 with active drag stowed.

A velocity versus time analysis was also conducted using the K2045Vmax-17 motor when active drag is stowed. The peak velocity, as shown by the OpenRocket simulations, is 720.49 ft/s using the K2045Vmax-17 motor. The plot of the OpenRocket simulation can be seen below in Figure 9.

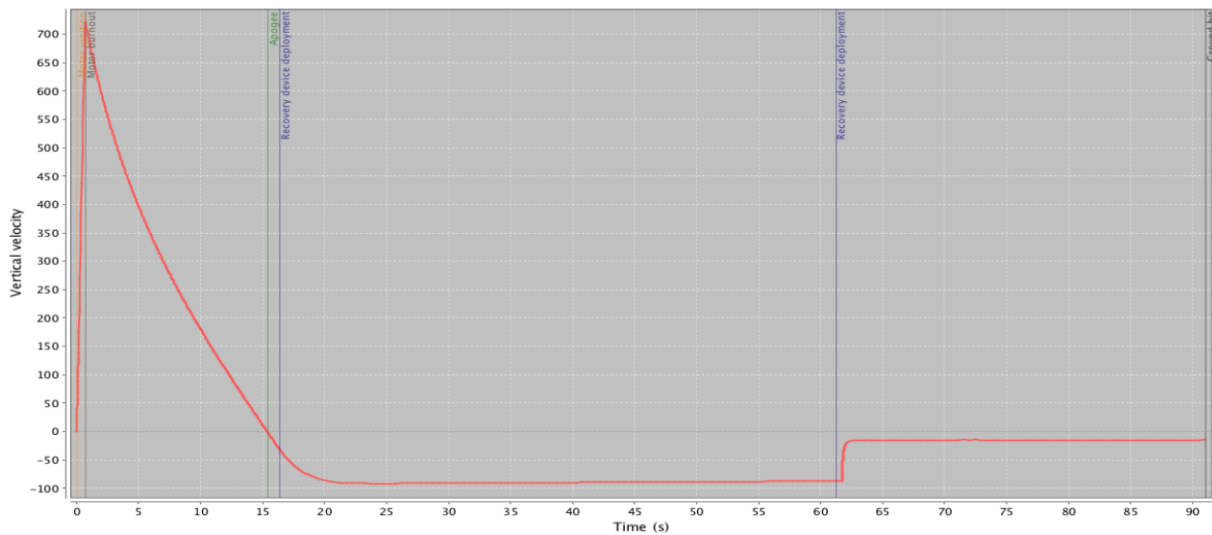


Figure 9. OpenRocket velocity simulation for the K2045Vmax-17 with active drag stowed.

A custom plot of the velocity versus time using the Cesaroni K2045Vmax-17 motor with active drag engaged is depicted in Figure 10.

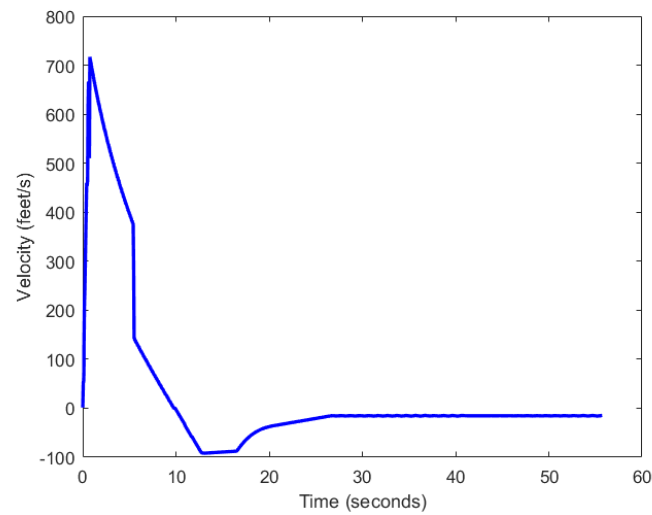


Figure 10. Custom velocity simulation for the K2045Vmax-17, with active drag engaged.

2.2.3 Estimated Drag Coefficient

Similar to the peak velocity estimations described in the previous section, the drag coefficient was calculated using both OpenRocket and the custom simulation. For the flight using the Cesaroni J295-16 motor, OpenRocket was used to simulate the coefficient of drag versus time, as can be seen in Figure 11 below. A custom simulation was not necessary for plotting these results, because the active drag is always stowed when using the J295-16 motor.

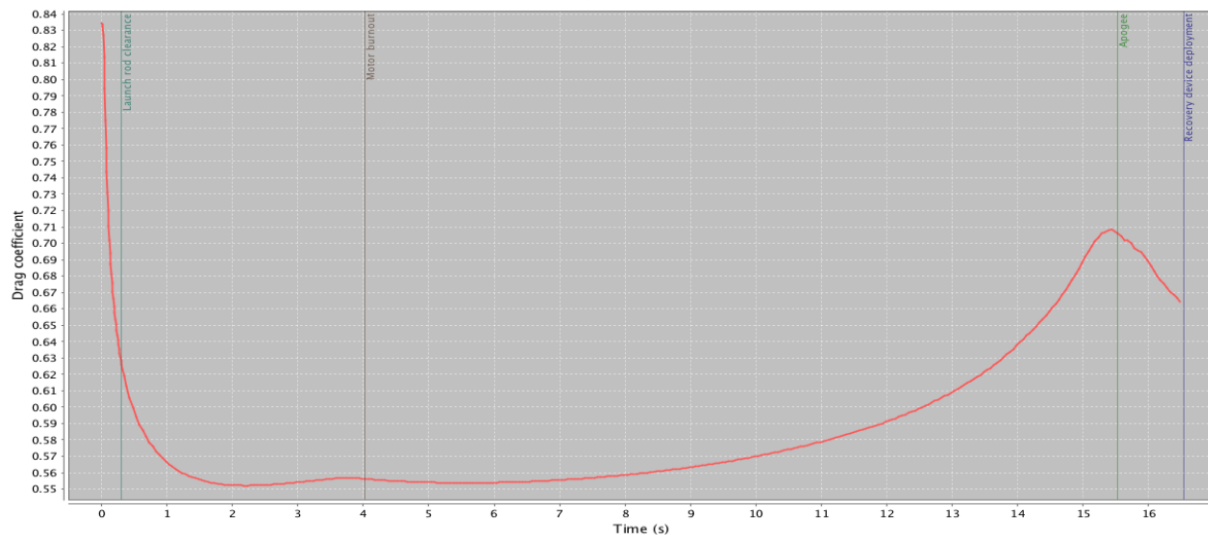


Figure 11. OpenRocket's coefficient of drag over time with active drag stowed using the Cesaroni J295-16 motor.

Using the K2045Vmax-17 motor, OpenRocket was used to analyze the drag coefficient when the active drag system was disengaged and is shown as a function of time in Figure 12.

The custom simulation was used to analyze the drag coefficient when the active drag was in use and is shown as a function of time in Figure 13.

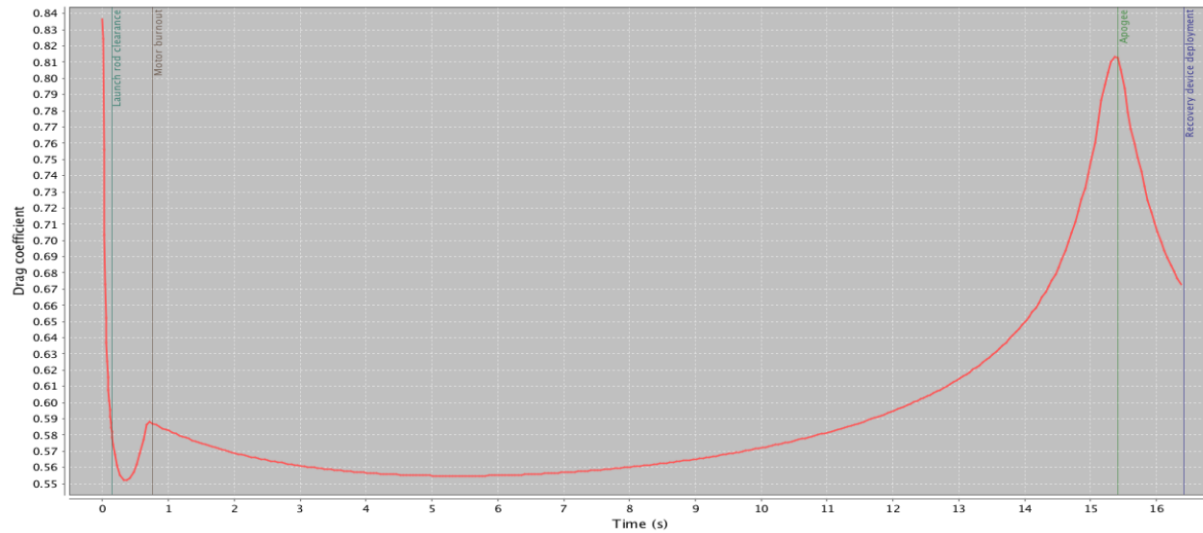


Figure 12. OpenRocket's coefficient of drag relative to time with active drag disengaged using the Cesaroni K2045Vmax-17 motor.

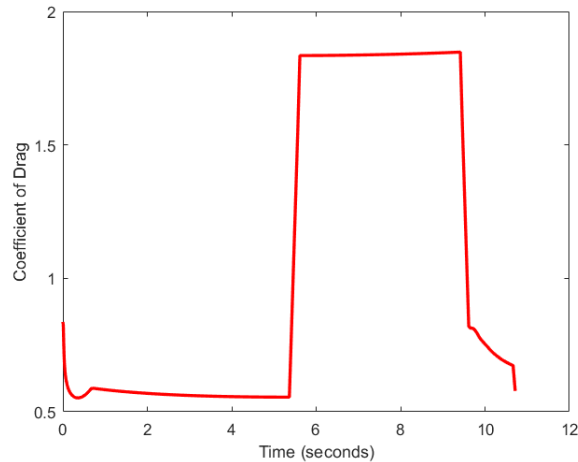


Figure 13. Custom Simulation Coefficient of Drag Over Time (Before Apogee), Active Drag Engaged using Cesaroni K2045Vmax-17 motor.

2.3 Recovery Analysis

In addition to the OpenRocket simulation data, terminal velocity calculations were completed by hand. The terminal velocity is calculated as

$$V_T = \sqrt{\frac{2mg}{\rho AC_d}} \quad (3)$$

where V_T is the parachute's terminal velocity, m is the mass of the components descending under the parachute, g is gravity, ρ is the air density, A is the frontal area, and C_d is the drag coefficient. Using Equation 3, the terminal velocity of both the main and drogue parachutes are calculated. For the drogue calculation with the J295 motor, the mass is found to be 12.33 lbm after subtracting the propellant, shock cord, and drogue parachute masses from the total mass. That Figure is 12.44 lbm with the K2045Vmax-17 motor, which is a negligible difference. The terminal velocity after deployment of the drogue parachute is 62.5 ft/s. For the main parachute calculation, the mass is found to be 11.07 lbm, which is the mass used for the drogue calculation minus the mass of the main parachute and shock cord. Using this mass, the terminal velocity after deployment of the main parachute is found to be 11.2 ft/s. This calculated velocity is acceptable as it is less than the maximum allowed descent rate of 24 ft/s.

It is also important that the vehicle does not descend too slowly as it will increase the drift distances and make retrieving the vehicle more difficult. All calculated values prove that our vehicle will be within range of safe decent speeds and will ease recovery of the vehicle post-launch. With our calculated descent velocities and predicted wind velocities, the vehicle's maximum drift is within reasonable distances.

2.4 Stability Analysis

OpenRocket was used to simulate stability margin caliber for the flight when the active drag is stowed. With the J295, the lowest stability margin is 1.87 and occurs at launch rail clearance at 0.31 s. This is still well above the minimum stability margin of 1.00 to fly safely. The highest stability margin is 3.03 and occurs at motor burnout. This stability margin is well below the maximum stability margin of 5 required for safe flight. With the K2045Vmax-17 motor, the lowest stability margin is 2.2 at .13s and the highest is 3.1 at motor burnout. After motor burnout the stability margin slowly decreases, until a sharp drop near apogee, where the stability margin drops to 1.1. This phenomenon is most likely a result of a discontinuity in the simulation, not the physical features of the rocket, and therefore not likely an accurate prediction for stability near to apogee. The values of the stability margin throughout the flight can be seen in Figures 14 and 15.

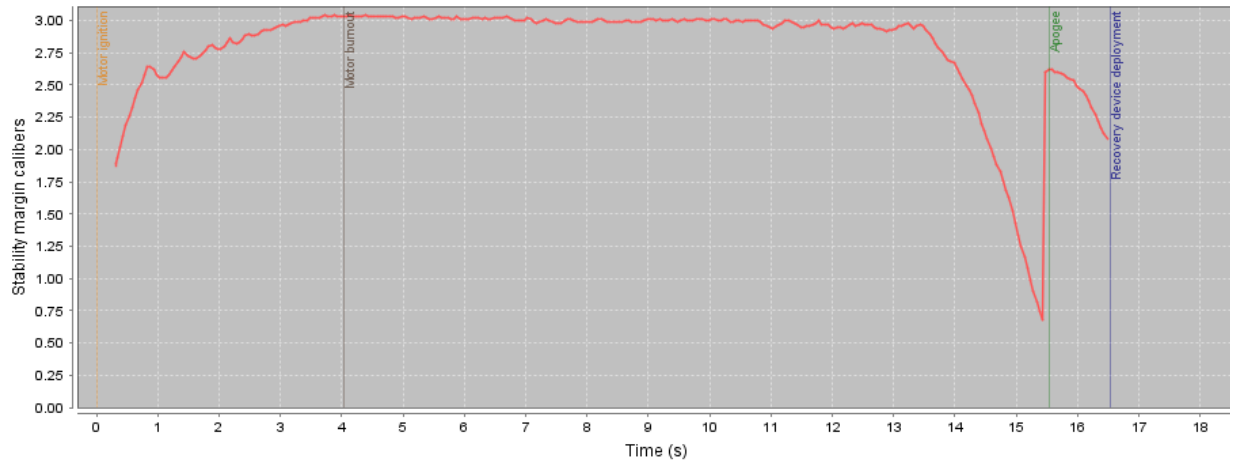


Figure 14. Stability margin calibers from OpenRocket for the J295-16.

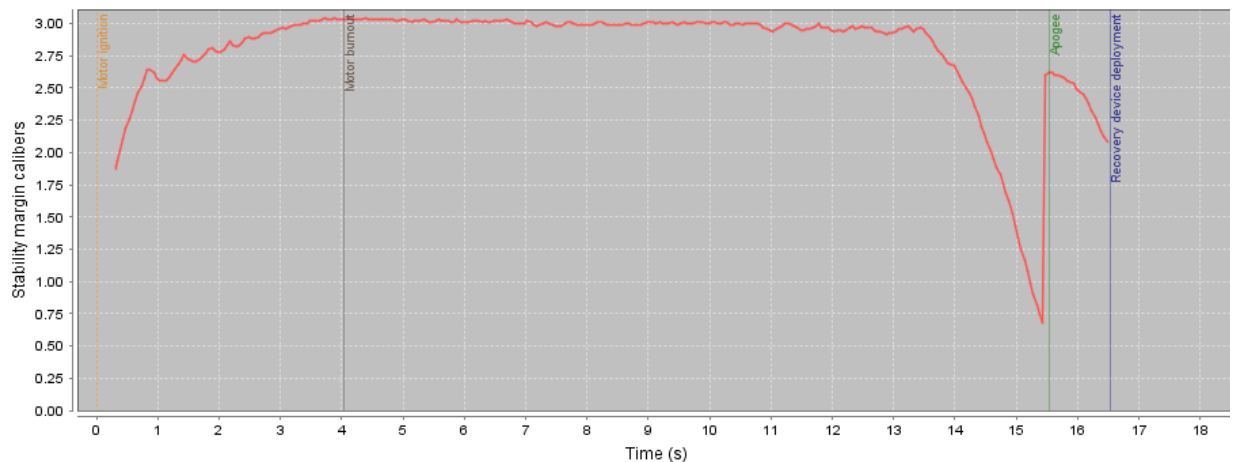


Figure 15. Stability margin calibers from OpenRocket for the K2045Vmax-17.

2.5 Environmental Conditions Analysis

When predicting the performance of the rocket prior to this point, a wind speed of 4.5 mph with 10% turbulence intensity in a direction perpendicular to vertical has been used in the simulations. Actual launch conditions will vary from the environmental conditions used in the simulation, either favorably or unfavorably. OpenRocket was used to simulate a 15 mph wind from the east, which would be a high wind speed for launch, to ensure flight is still safe. With 15 mph wind, the rocket will drift 300 ft west, which is not too large a distance for drift given high wind speeds. The evenness of the launch site could pose the risk of not launching vertically. The team will check the evenness of the ground before launching and check the angle of the rocket on the launch rail with a level to verify that the rocket will launch in the desired direction.

The effect of the rocket on the environment must also be considered and precautions must be taken to minimize any potential damage. Starting at launch, it is possible that the heat or

exhaust from the motor could damage the ground. This can be reduced by ensuring that there is an adequate blast shield in place. Another risk is that the rocket lands hard and damages the ground on impact. The team has taken this risk into account during design and has made sure that the descent rate is well below any speeds that would cause damage to either the ground or the rocket. If parts were to come loose during launch or landing and were left there, it would be damaging to environment. The team will check the rocket after recovery for any missing parts, and those missing parts (if there are any) will be located and removed.

3. SAFETY

3.1 Flight and Recovery Safety

The rocket has been designed with safety in mind at all times, especially during the flight and recovery processes. During launch, the speed of the rocket when it is 6 ft up the rail far exceeds the minimum requirement for a safe launch. Similarly, the exit velocity of the rocket off the rail is greater than the minimum speed requirement, allowing for a stable, vertical flight and minimizing risk due to an unpredictable flight path. The parachutes will be deployed at appropriate times to ensure that the landing speed is safely under 24 ft/s. A radio tracker will allow the team to locate the rocket after flight in a timely manner, ensuring an efficient launch and recovery.

3.2 Material-Handling Procedures

Hazardous materials will be used during construction, testing, and launch of the rocket so proper handling of these components is imperative. Materials that present the greatest hazards are the flammable motor, epoxy, black powder charges, and fiberglass, all materials with which at least one team member has experience. The experienced team member(s) will teach the rest of the team the proper handling techniques and safety procedures; they will also oversee the team's use of these materials.

Flammable materials will always be handled according to their specific instructions and will be carefully kept away from any source of open flame or other potential spark. A fire extinguisher will be kept on hand at all times. Gloves will be worn whenever the team is working with epoxy or other potential skin irritants. Any parts that have been epoxied and are drying will be labeled as such and kept in a separate area to avoid any accidental contact with the chemicals. Black powder will be stored carefully and according to specifications; extra precautions will be taken when measuring to ensure precision. Fiberglass will always be handled with gloves to avoid splinters and masks will be worn during cutting to avoid inhalation of fumes or particles. Safety glasses will be on hand at all times for protection as necessary.

3.3 Assembly Procedures

Due to the assembly time constraint during the day of the launch, team members must learn and practice the assembly procedures prior to the competition in order to avoid mistakes that would compromise safety. Before the competition, the team will carefully go over the

assembly of the rocket to ensure that everyone understands and can complete all of the steps. Team members will practice the construction until assembly can be accomplished in under an hour. A checklist will be made of all of the steps and parts necessary for assembly as a guide to ensure that no step is skipped or performed out of order and that no part is left out. With practice, the checklist should become superfluous, but will be kept on hand as a safety precaution. Each team member will be assigned certain tasks to streamline the assembly process, but all team members will be capable of completing every step in case a member is absent during the launch.

3.4 Pre- and Post-Launch Procedures

Prior to and after launch of the rocket, team members will take precautions and adhere to the predetermined procedures and safety codes. The team will first go through all of the components and ensure that each part is present and in working condition. After the preliminary check, the team will begin assembly of the rocket, taking extra care to implement all of the parts safely and securely. The team will then survey the launch area to account for any unevenness in the ground and counteract it to ensure a safe, vertical flight. Once launch is complete, the team will scan the area to confirm that it is safe and then recover the rocket. The aforementioned radio tracker in the rocket will allow the team to quickly locate the rocket. Upon finding the rocket, the team will check for any parts that may have come loose during flight, or on impact, and secure them before bringing the rocket back to the setup area. At this point, the team will then begin the procedure again for the second flight.

4. TEST FLIGHTS

4.1 Model Rocket Demonstration Flight

The model rocket, an Aerotech Barracuda, was flown on November 12, 2016 during a Central Illinois Aerospace launch in Champaign, IL. The model launch was to demonstrate the team is capable of building, assembling, successfully launching and recovering a rocket. Figure 16 shows the rocket being prepared for launch on the launch rail. Figure 17 shows the team with the rocket prior to launch. The rocket was successfully recovered post-launch.



Figure 16. Rocket being prepared for launch.

Figure 17. Team picture prior to launch.

4.2 Test Flight Plan

The test flight will take place on April 8th, 2017 in Rantoul Aviation Center through Central Illinois Aerospace. The rocket will be launched twice, using both intended competition motors. One launch will be with the J-295 motor without utilizing the active drag. The second launch will be with the K2045Vmax-17 motor with the active drag utilized during flight. All competition avionics will be in place so as to best simulate competition conditions during the test flights. This launch will also be an opportunity for the team to practice assembling the rocket in under an hour, as is required during the competition. The data between the two launches will be compared to determine how effective the active drag is in slowing down the rocket with the K2045Vmax-17 motor, how close the apogees between the two flights are, and how accurate the velocity measurement system is. This analysis will allow the team to make necessary changes to the active drag and velocity measurement systems to increase its performance before the competition.

5. BUDGET

The project budget can be seen below in Table 4. It includes all purchased parts, the competition registration fee, and estimated travel costs.

Table 4. Proposed Budget

Component	Price
Nose cone	\$21.95
Blue Tube	\$77.90
Coupler	\$21.90
Bulkheads	\$17.50
Main parachute	\$105.00
Drogue parachute	\$56.90
Parachute protectors	\$16.30
Epoxy	\$38.25
Epoxy pumps	\$5.94
Centering rings	\$17.02
Motor mount tube	\$23.95
Fiberglass	\$81.00
Eye bolts	\$21.12

Balsa wood	\$9.00
Stratologger altimeter	\$49.46
Raven3 altimeter	\$155.00
Rail buttons	\$4.65
Motor casing	\$84.69
Rear closure	\$42.75
Motor retainer	\$31.03
Aft closure	\$48.15
K2045Vmax-17 motor	\$113.94
J295-16	\$91.50
Terminal blocks	\$10.23
Shear pins	\$9.30
Switches	\$29.79
Pitot Probe	\$8.49
Paint	\$13.96
Ejection charge canister caps	\$6.30
Pressure transducer	\$80.00
Solenoids	\$35.00
Torsion Spring	\$10.00
Aluminum rods	\$14.00
Quick links	\$5.40
Registration fee	\$400.00
Travel Costs	\$1000.00
Total project Cost	\$2657.37